NASA Contractor Report 191447
ICASE Report No. 93-15

P-21

ICASE

20 Years of Excellence

GODUNOV-TYPE SCHEMES APPLIED TO DETONATION FLOWS

James J. Quirk

NASA Contract No. NAS1-19480
April 1993

Institute for Computer Applications in Science and Engineering
NASA Langley Research Center
Hampton, Virginia 23681-0001

Operated by the Universities Space Research Association

National Aeronautics and
Space Administration

Langley Research Center
Hampton, Virginia 23681-0001

GODUNOV-TYPE SCHEMES APPLIED TO DETONATION FLOWS

James J. Quirk[1]

Institute for Computer Applications in Science and Engineering
Mail Stop 132C, NASA Langley Research Center
Hampton, Virginia 23681

ABSTRACT

Over recent years, a variety of shock-capturing schemes have been developed for the Euler equations of gas dynamics. During this period, it has emerged that one of the more successful strategies is to follow Godunov's lead and utilize a nonlinear building block known as a Riemann problem. Now, although Riemann solver technology is often thought of as being mature, there are in fact several circumstances for which Godunov-type schemes are found wanting. Indeed, one inherent deficiency is so severe that if left unaddressed, it could preclude such schemes from being used to capture detonation fronts in simulations of complex flow phenomena. In this paper, we highlight this particular deficiency along with some other little known weaknesses of Godunov-type schemes, and we outline one strategy that we have used to good effect in order to produce reliable high resolution simulations of both reactive and nonreactive shock wave phenomena. In particular, we present results for simulations of so-called galloping instabilities and detonation cell phenomena.

[1]Research was supported by the National Aeronautics and Space Administration under NASA Contract No. NAS1-19480 while the author was in residence at the Institute for Computer Applications in Science and Engineering (ICASE), NASA Langley Research Center, Hampton, VA 23681.

1. Introduction

Following the rise of computational fluid dynamics, numerical simulations of shock wave phenomena are now commonplace. Such simulations are attractive as replacements for experiments which are either difficult, dangerous, or expensive, and can be done for problems which are not amenable to analytical methods. However, because of the disparate scales involved, simulations are all too often under-resolved and so are of limited use. Indeed, despite the plethora of numerical schemes that have been developed, only the Godunov-type methods have been shown to produce, genuinely, high fidelity simulations of complex shock wave phenomena (Berger and Colella, 1989; Quirk, 1992 *a*). Consequently, following a survey of the literature, Godunov-type methods are likely to be picked up by people who are not algorithm developers as tools with which to simulate real problems. Unfortunately, despite their undoubted strengths, Godunov-type schemes have certain inherent weaknesses that can, occasionally, result in simulations failing catastrophically. Amongst the cognoscenti, such weaknesses, whilst not always fully understood, can be overcome. However, the non-expert is severely disadvantaged by the fact that the various failings and their associated fixes go largely unreported. Recently we have attempted to redress this unfortunate state of affairs (Quirk, 1992 *b*), and here we present an abridged version of this work which is targeted directly at people within the combustion community who would like to take advantage of modern shock-capturing schemes for simulating detonation flows.

The rest of this paper is as follows. In Section 2 we present a brief outline of Godunov-type schemes. This is followed by a section containing some specific examples of how different schemes can fail. In Section 4 we describe the strategy that we use to improve the robustness of our flow solvers, following which, we present results for simulations of galloping instabilities and detonation cell phenomena. Finally, in Section 6 we present some conclusions that we have drawn from this work.

2. Outline of Godunov-type Schemes

Many expositions of Godunov's method and its descendants appear in the literature (Holt, 1984; Roe, 1986); here we simply want to present the general gist of such schemes in order to orientate the reader for the material which follows in the remaining sections of this paper.

With reference to Figure 1, a Godunov-type scheme may be viewed as follows. The scheme works with a low-order projection of the flow solution; each mesh cell contains a cell-averaged value for the true solution over the cell. Thus, the numerical representation closely approximates the true solution near discontinuities, and regions of smooth flow are reasonably well approximated by a series of step functions. This discrete system is integrated by first reconstructing the flow solution within each cell. This step is effectively an extrapolation process for finding the flow states at the edges of mesh cells given values at the centres of cells. Note that, in general, the reconstructed solution whilst smoother than the projected solution will still be discontinuous at cell interfaces. Next there comes an evolution step. A Riemann problem is solved for each cell interface using the reconstructed

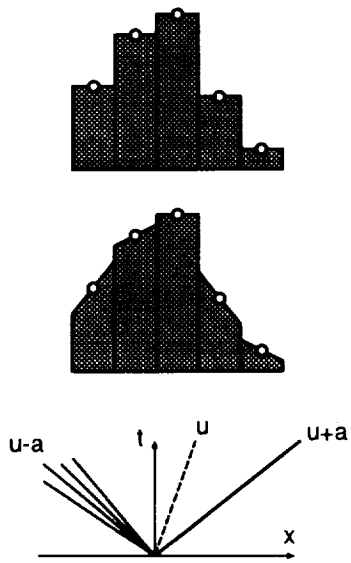

Cell-averaged projection of the flow solution.

Piecewise-linear reconstruction of the flow solution.

Typical Riemann solution showing three centred waves.

Figure 1: A Godunov-type scheme consists of three basic steps: *reconstruction→evolution →projection*.

states on either side of the interface as input data. Recall that the Riemann problem for any set of conservation laws arises, if initial data are prescribed as two semi-infinite states ($\mathbf{W} = \mathbf{W}_L$ for $x < 0$, $\mathbf{W} = \mathbf{W}_R$ for $x > 0$). The solution to a Riemann problem consists of a number of centred waves. For the one-dimensional Euler equations of gas dynamics there are three waves. The inner wave is a contact discontinuity separating states at different temperatures, and each of the two outer waves may be either a shock wave or an expansion wave. Finally, the different solutions to the separate Riemann problems are averaged so as to find a cell-centred projection of the flow solution at some new time level. If repeated, the sequence *reconstruction→evolution →projection* results in an accurate and well-behaved scheme for simulating the propagation of shock waves.

Whilst the overall strategy of a Godunov-type scheme is largely clear-cut[2], the same cannot be said of its individual components. For example, more often than not, the Riemann problem for a system of conservation laws does not have an analytic solution and is therefore expensive to compute. Consequently, many workers prefer to compute an approximate solution to the Riemann problem which embodies the spirit of the exact solution but which is cheaper to compute (Roe, 1986; Einfeldt, 1988; Toro, 1991). Indeed, the design of approximate Riemann solvers has become something of an industry in its own right, and there is considerable debate concerning the relative merits of different solvers. Moreover, there are

[2]Here we have described the so-called MUSCL approach for producing a high-order Godunov method. An alternative methodology is followed by flux-limited schemes where the reconstruction step is replaced by a procedure which post-processes the Riemann solution.

many circumstances for which certain approximate solvers actually prove to be more reliable than the exact solver. Therefore, in general, it is far from obvious which particular Riemann solver is best suited to a given application.

The reconstruction step is similarly open to different interpretation. Firstly, there is a free choice as to which variables are reconstructed, and which quantities are derived from the reconstructed variables. For example, although shock capturing schemes invariably work with the conserved variables, experience shows, at least for the Euler equations, that better results are obtained if the reconstruction is performed using primitive variables. Secondly, there is also a choice as to the order of accuracy of the reconstruction. As is common practice, we employ piecewise-linear slopes (Quirk,1992 *a*); however, Colella and Woodward (1984) use piecewise-parabolas to good effect in their PPM scheme, and more recently Harten *et al.* (1987) have introduced the idea of ENO schemes where the reconstruction step may be carried out to some arbitrary order of accuracy.

It is worth noting, however, that to a large extent the quality of results produced will depend on how well the flow solution is reconstructed near discontinuities and so the notional order of accuracy for some reconstruction process is not necessarily a reliable indicator of its actual performance. Typically, limiter functions (Roe, 1985) are employed so as to ensure that the reconstruction process does not introduce unwanted overshoots near extrema, and it is the properties of the chosen limiter function that largely dictate the quality of the flow solution. But a limiter function is only as good as the data upon which it acts. For example, although we employ a piecewise-linear reconstruction which results in a scheme that is nominally only second-order accurate, the slopes are derived from the Riemann solutions which are computed using the cell-centred states as input data. For very high resolution simulations which involve thousands of time steps, this strategy gives markedly better results for weak discontinuities such as contact surfaces than does the third-order reconstruction process proposed by Anderson *et al.*(1985) which does not utilize the same level of characteristic information. While the differences are much less marked for problems that contain just a few time steps, they are still appreciable (see Figure 2).

Everything considered, given the basic framework of a Godunov-type scheme, it is possible to construct many different variations on a theme. Unfortunately, there is no "correct" way of doing things, for the theory which underpins this class of scheme does not always discriminate between the different options that are available. In practice, seemingly innocuous details of the reconstruction process can have a large bearing on the quality of the results produced for the sorts of very detailed simulations that will be necessary in order to unravel the dynamics of detonation phenomena. Thankfully, the large scale flow features are normally insensitive to such changes, and so one's faith in Godunov-type schemes is not unduly undermined by the uncertainties in the precise details of the method.

Before proceeding to the next section which exposes some of the failings of Riemann solvers, so as not to appear to paint an overly pessimistic view of the capabilities of Godunov-type schemes, it is worthwhile showing what can be achieved if due care is taken. Figure 3 shows a snapshot taken from the simulation of a planar shock wave diffracting around a 90^o corner (Quirk, 1992 *b*). This picture is similar to a Schlieren image in that the different

(a)

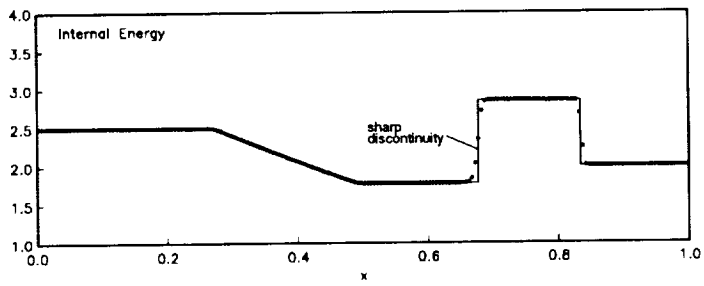

(b)

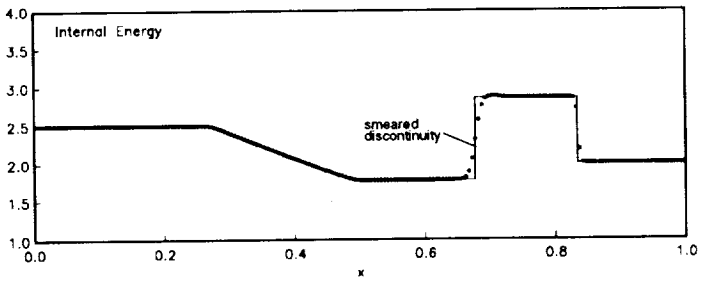

Figure 2: The internal energy profiles computed for Sod's problem using: (a) 2^{nd} order characteristic MUSCL (Quirk, 1992)., (b) 3^{rd} order non-characteristic MUSCL (Anderson *et al.*, 1985).

shades of grey depict the magnitude of the gradient of the density field (the darker the shade, the larger the gradient), and it clearly shows all the salient flow features as identified experimentally by Bazenhova *et al.* (1984).

Briefly, with reference to Figure 4, the diffraction of the incident shock wave (AC) around the corner gives rise to an expansion fan which emanates from (O). The shape of this fan's lead characteristic (AQO) indicates that the flow upstream of the incident shock is supersonic. The expansion fan interacts with the incident shock to form the disturbed shock front (ADMN). The incident shock is sufficiently strong that this disturbed front is kinked; a Mach reflection at the wall gives rise to a triple point at (M). A contact surface (ALO) marks the boundary between fluid that has been induced into motion by the incident shock and fluid which has been processed by the disturbed shock front. Note that the flow is separated from the wall at a point slightly downstream of the apex of the corner, and a slipstream (OS) separates the expanded flow from this region of almost stationary gas. The free end of this slipstream rolls up into a vortex. A secondary shock wave (KTS) matches the pressure of the flow accelerated by the expansion fan to that of the decelerated flow behind the disturbed part of the incident wave. This secondary shock is kinked as a result of its interaction with the slip stream (OS). A secondary contact surface (TL) begins at the point of intersection of the secondary shock wave with the weak shock (OT) which terminates the expansion fan. Lastly, a shock wave (PB) is present so as to decelerate the reversed flow within the separated region as it approaches the point of diffraction.

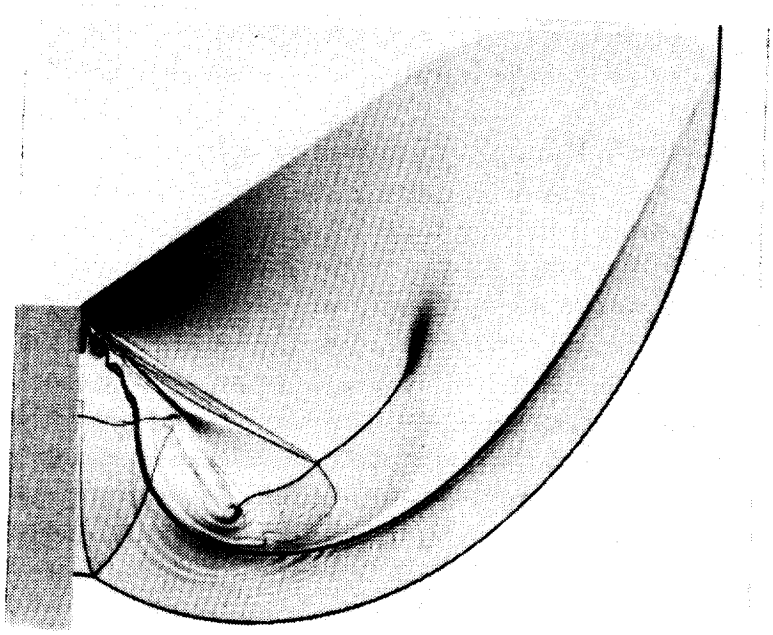

Figure 3: A numerical Schlieren-type image taken from the simulation of a planar shock wave diffracting around a 90° corner.

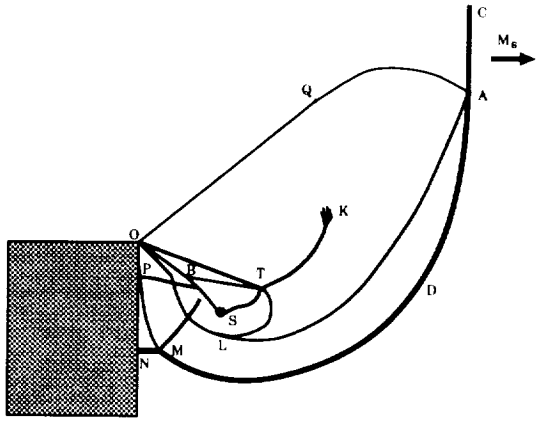

Figure 4: Schematic showing the main flow features of the above Schlieren-type image.

3. Some Failings of Riemann Solvers

We now present some examples where certain Riemann solvers are known to give unreliable results for the Euler equations of gas dynamics. Whilst our catalogue of failings is not exhaustive, it should alert the reader to the types of problems that they might encounter when using Godunov-type methods. It is important to realise that no one failing afflicts all Riemann solvers. Conversely, however, it would appear that no one Riemann solver is completely free of defects.

With reference to Figure 5, Example (a) shows how spurious post-shock oscillations can occur whenever a shock wave moves very slowly during the course of a simulation. Here, a one-dimensional shock wave is moving from left to right (for a Courant number of one, it takes approximately 50 time steps for the shock to traverse a single cell). As the shock moves relative to the mesh, so the smeared numerical shock profile inevitably changes shape. Unfortunately, for many Riemann solvers including the exact solver, the points within the smeared profile do not lie on the Hugoniot curve connecting the pre-shock state to the post-shock state. Thus these two states cannot be connected by a single family of acoustic waves. For such schemes, whenever the shock profile changes, so the supposedly passive wave fields are activated (in this case, the u and $u - a$ wave fields), thus giving rise to low frequency oscillations. A thorough description of this particular failing has been given by Roberts (1990). Note that these oscillations are not the same as the high-frequency, post-shock oscillations that afflict finite-difference shock-capturing schemes.

Example (b) in Figure 5 is taken from a simulation of double Mach reflection which was performed using Roe's scheme; here we show a snapshot of the pressure contours at one instant in time. The Mach stem is inexplicably kinked giving rise to a spurious triple point (S). It should be noted that this kinking is not related to the slight bulging that is often observed experimentally for this type of shock reflection problem. Such bulging arises because the contact discontinuity emanating from the primary triple point is deflected by the reflecting surface resulting in a strong wall jet which effectively pushes out the base of the Mach stem. The mechanism behind this failing is not fully understood, but it would appear to arise from the fact that the Mach stem is closely aligned with the computational grid. Consequently, little or no dissipation is provided by Roe's scheme, in a direction parallel to the stem, to control the kinking.

Generally speaking, the dissipation mechanism provided by many Riemann solvers proves to be inadequate whenever a strong shock wave is aligned with the computational grid. Example (c) shows the so-called carbuncle phenomena (Peery and Imlay, 1988) where some schemes fail to produce a realistic bow shock for a blunt body placed in a high Mach number flow (here we have plotted density contours). Note that along the stagnation line the bow shock is more or less aligned with the body-fitted grid used for the calculation, and so very little dissipation is added normal to the stagnation line in the vicinity of the bow shock; a small amount of auxiliary dissipation applied in this region is generally sufficient to suppress the carbuncle.

Example (d) in Figure 5 shows a particularly insidious failing that can occur when a strong shock is aligned with the grid. Here we have plotted a single snapshot of the density

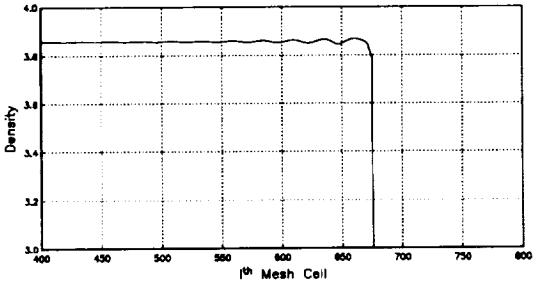

(a)

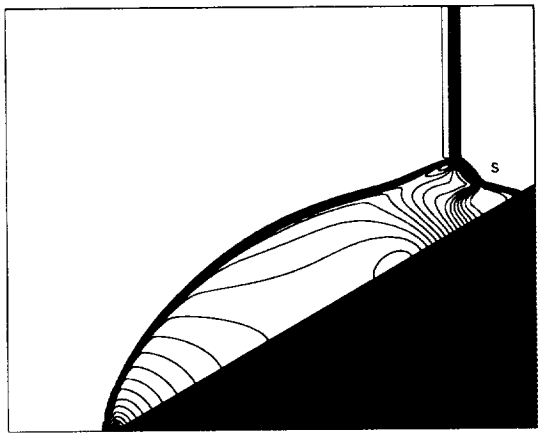

(b)

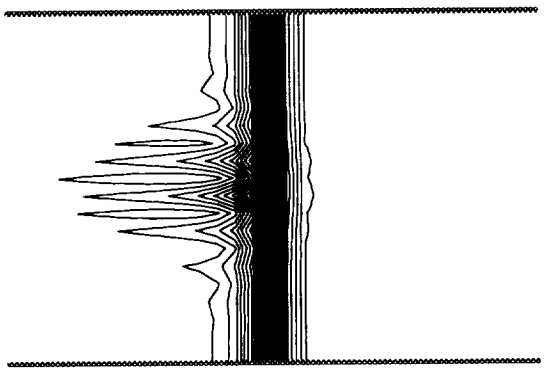

(d)

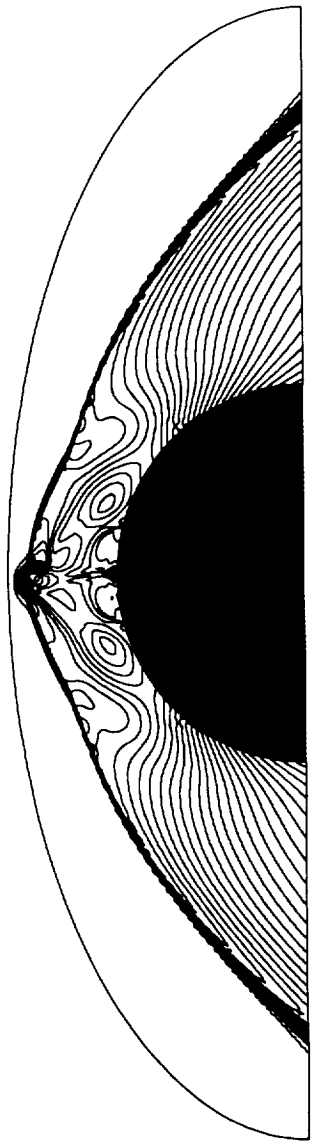

(c)

Figure 5: Some Riemann solver failings: (a) Slowly moving shocks., (b) Kinked Mach stems., (c) The Carbuncle phenomena., (d) Odd-Even decoupling.

contours taken from the simulation of an initially planar shock wave which is propagating down a duct, from left to right. A nominally uniform Cartesian grid was used for the calculation; the grid centre-line carried a small saw-tooth perturbation. This perturbation acts like a forcing function which causes odd-even decoupling to occur, along the length of the shock, in both the density and pressure fields. Interestingly, within the body of the shock, the decoupling of the density field is out of phase with that of the pressure field. An attempt to explain this failing has been given by Quirk (1992 *b*), but certain details of the mechanism remain unclear. It is clear, however, that this numerical instability only occurs for strong shocks, and that it takes a long time to develop (here, the shock had propagated approximately thirty channel widths before the instability first became apparent). Moreover, as will be shown in Section 5, this particular instability has quite grave consequences for the simulation of two-dimensional detonation fronts; waves produced by the numerical instability can interfere with the genuine transverse waves associated with the propagation of the front.

For many problems, the nature of the flow solution is known *a priori*, and so it is fairly obvious whenever a simulation gives anomalous results. But often no such safety net exists, in which case it becomes very difficult to determine the fidelity of a numerical simulation. One tactic that we routinely employ is to run a simulation two or more times, each time varying the elements of the flow solver. For example, we may change our choice of Riemann solvers, or we may change our choice of variables for the reconstruction process. Admittedly, the fact that two such simulations give similar behaviour is no guarantee that the results are correct, but it is useful for determining which features of the solution are likely to be numerical artifacts. Lastly, it should be noted that many of the failings associated with Godunov-type methods could be circumvented if strong shocks were fitted rather than captured. However, given the complexity of a general purpose shock-fitting scheme, this option is not likely to appeal to the worker who is merely using a Godunov-type scheme as a tool.

4. An Adaptive Riemann Solver

Having exposed some of the weaknesses of Riemann solvers, we now present a simple strategy, that we have found useful, for improving the all-round robustness of Godunov-type schemes. In essence, we select the precise flavour of upwinding to match the local flow data such that a particular Riemann solver is only employed in those situations where it is known to give reliable results. By recognizing the limitations of any one solver it is possible to reap its advantages without suffering its attendant failings.

Our synergetic strategy has a number of attractions, not least of which is that some favoured solver need not be jettisoned simply because it, occasionally, fails. However, it does introduce the difficulty of how to decide when to use one Riemann solver in preference to another. But it has been our experience that this added difficulty is not particularly bothersome, for we tend to combine a single high resolution Riemann solver with just one or two other solvers that prove more reliable under conditions which are fairly well-defined, and so a set of *ad hoc* switching functions suffice. For example, some of the worst failings

of Riemann solvers occur in the vicinity of strong shock waves. To overcome such failings we use the HLLE scheme (Einfeldt, 1988). Now it makes little sense to chop and change the choice of Riemann solver used along the length of a shock wave, since to do so would inevitably perturb a planar shock front. Hence, we apply this particular Riemann solver throughout the immediate vicinity of a strong shock. Thus the HLLE switching function need only locate the position of a shock wave, but such functions already exist in the guise of mesh refinement, monitor functions.

A simple test that identifies those cell interfaces which are in the vicinity of a strong shock is to check whether or not

$$\frac{|p_r - p_l|}{min(p_l, p_r)} > \alpha, \tag{1}$$

where α is some threshold parameter which is problem dependent and p_r and p_l refer to the pressures which act on the interface. If this condition is met, the two cells separated by the interface are flagged as lying within a strong shock. Then, when it comes to computing cell-interface fluxes, if the cells either side of an interface have both been flagged as lying within a strong shock, the flux is computed using the HLLE solver. Note that since numerical shocks are invariably smeared over several mesh cells, it is worth locating shocks using a projection of the flow solution on a grid which is coarser than that used for the calculation. On such a grid a shock will appear much less smeared, and so the left-hand side of the above switching function will be a fair indication of its strength. Once a set of cells have been flagged on this coarse mesh, the flags may be prolongated to the actual computational mesh so as to find those cells which lie in the vicinity of a shock wave.

Figure 6 shows how the HLLE solver may be used to correct the tendency of Roe's scheme to produce kinked Mach stems, c.f. Figure 5 (b). For this calculation the HLLE switching function was tuned such that it would only be activated by the incident shock, and the principal Mach stem; the threshold parameter α was simply set to half the strength of the incident shock wave as given by the left-hand side of Equation 1. Note that apart from the region near the Mach stem, these new results are very similar to the old ones. This shows that the HLLE scheme has had no adverse affect on the resolution of Roe's scheme.

Having presented the gist of our strategy, we see little point in trying to sell a particular combination of solvers. Starting with some high resolution Riemann solver, whose choice will inevitably be a matter of personal taste, the correct combination of solvers will depend both on that schemes weaknesses and on the specific application in hand. In turn, the combination of Riemann solvers will dictate the choice of switching functions.

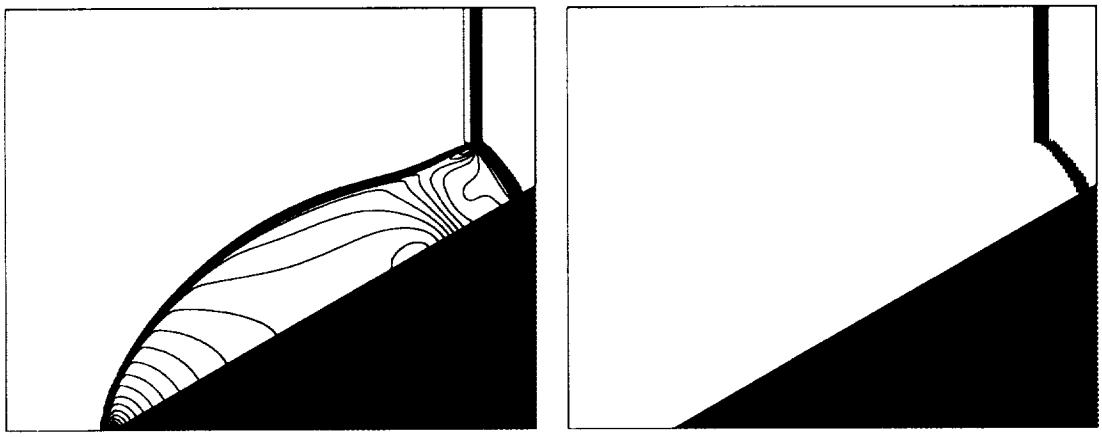

(a) (b)

Figure 6: The HLLE scheme can be used to circumvent the tendency of Roe's method to produce kinked Mach stems: (a) Pressure Contours, (b) HLLE switching function.

5. Galloping Instabilites and Detonation Cells

Almost all of our experience with Godunov-type schemes has been gained from calculations of nonreactive flows. However, as will be shown in this section, the basic lessons that we have learnt remain important when it comes to performing simulations of detonation phenomena. Thus far, for simplicity, we have utilized the so-called Reactive Euler equations for our detonation simulations; a single reactant A is converted to a single product B by a one-step irreversible chemical reaction which is governed by Arrhenius kinetics.

In one space dimension the reactive Euler equations may be written in non-dimensional form as

$$\frac{\partial}{\partial t}\begin{pmatrix}\rho\\ \rho u\\ E\\ \rho Z\end{pmatrix}+\frac{\partial}{\partial x}\begin{pmatrix}\rho u\\ \rho u^2+p\\ (E+p)u\\ \rho u Z\end{pmatrix}=-\begin{pmatrix}0\\ 0\\ 0\\ K\rho Z\exp^{-E^+/T}\end{pmatrix} \tag{2}$$

Here ρ, u, p, T, E, Z and E^+ are the density, velocity, pressure, temperature, total energy per unit volume, reactant mass fraction, and the activation energy, respectively. Note that K is a free parameter that simply sets the spatial and temporal scales. Typically, K is chosen such that for a ZND wave the half-reaction length (the distance behind the detonation front by which point half of the reactants have been consumed) is scaled to unit length. The

following equations are used to close the system (2)

$$\begin{aligned} E &= \rho e + \rho q Z + \tfrac{1}{2}\rho u^2, \\ p &= (\gamma - 1)\rho e, \\ T &= p/\rho. \end{aligned} \tag{3}$$

Here e is the specific internal energy, γ is the ratio of specific heats and q is the heat release parameter for the chemical reaction $A \rightarrow B$.

We integrate the above system of equations, which are of the form $\frac{\partial \mathbf{w}}{\partial t} + \frac{\partial \mathbf{f}}{\partial x} = \mathbf{s}$, using the method of fractional steps

$$\mathbf{w}^{n+2} = \mathcal{L}_s.\mathcal{L}_c.\mathcal{L}_s.\mathbf{w}^n$$

The source operator, $\mathcal{L}_s$, corresponds to integrating $\frac{\partial \mathbf{w}}{\partial t} = \mathbf{s}$, which in this case reduces to integrating the single ODE, $\frac{dZ}{dt} = -KZ\exp^{E^+/T}$. We assume that the temperature field is frozen for this step, allowing us to use the nominally exact operator

$$Z^{n+1} = Z^n \exp(-K\exp(-E^+/T^n)\Delta t),$$

where Δt is the time step going from time level n to time level $n+1$. For the convective operator, $\mathcal{L}_c$, which corresponds to integrating $\frac{\partial \mathbf{w}}{\partial t} + \frac{\partial \mathbf{f}}{\partial x} = 0$, we employ Hancock's finite-volume scheme (Quirk, 1992a) in conjunction with the adaptive Riemann solver outlined in this paper. Note that the convective operator uses a time step that is twice as large as that used by the source operator. The generalization of this integration strategy to two space dimensions simply consists of replacing the one-dimensional convective operator by its two-dimensional counterpart.

To assess the capabilities of our scheme we have performed simulations of one-dimensional pulsating detonations, or so-called galloping instabilities, for which bench-mark results appear in the literature (Fickett and Wood, 1966; Bourlioux *et al.*, 1991). Here we limit ourselves to presenting the case where the overdrive is 1.6 and the dimensionless parameters that appear in equations (2) and (3) are given by: $\gamma = 1.2$, $E^+ = 50$, $q = 50$ and $K = 230.75$. We have run this problem using several different mesh resolutions in combination with several different approaches for performing the reconstruction step of our Godunov-type scheme. Figure 7 shows the shock pressure history for the case where the computational grid provided 40 mesh cells per half-reaction length, and the reconstruction process operated on a characteristic decomposition of the conserved variables. Qualitatively, this pressure trace is identical in form to that presented by Bourlioux *et al.* (1991) which was found using a scheme that fitted rather than captured the detonation front. Figure 8 shows a convergence study for the variation of the peak shock pressure with mesh spacing for two popular limiter functions, namely Superbee and Minmod (Roe, 1985), in both cases the reconstruction process operated on the conserved variables. Note that a relative mesh spacing of 1 corresponds to having 10 cells per half-reaction length, and so 0.125 corresponds to having 80 cells per

half-reaction length. Pleasingly, the grid-converged value for the peak pressure is independent of the reconstruction process. Moreover, it is in close agreement with the value given by Fickett and Wood (1966), and the value found by extrapolating the results of Bourlioux *et al.*(1991).

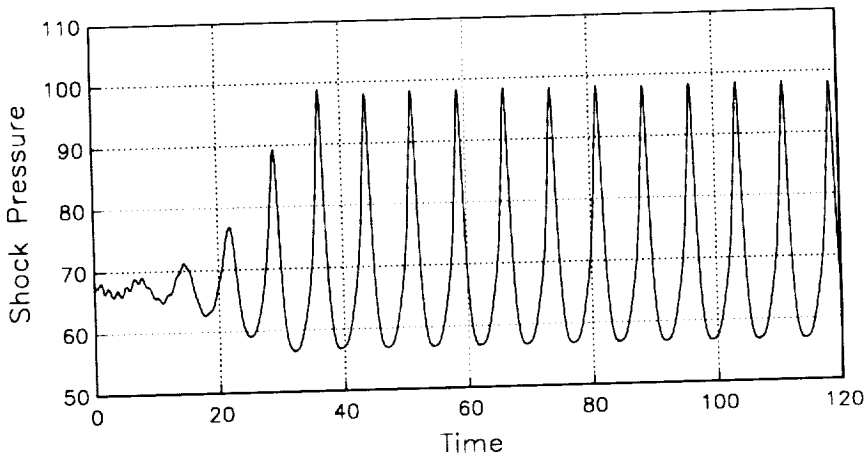

Figure 7: Shock pressure history trace for a calculation with 40 mesh cells per half-reaction length.

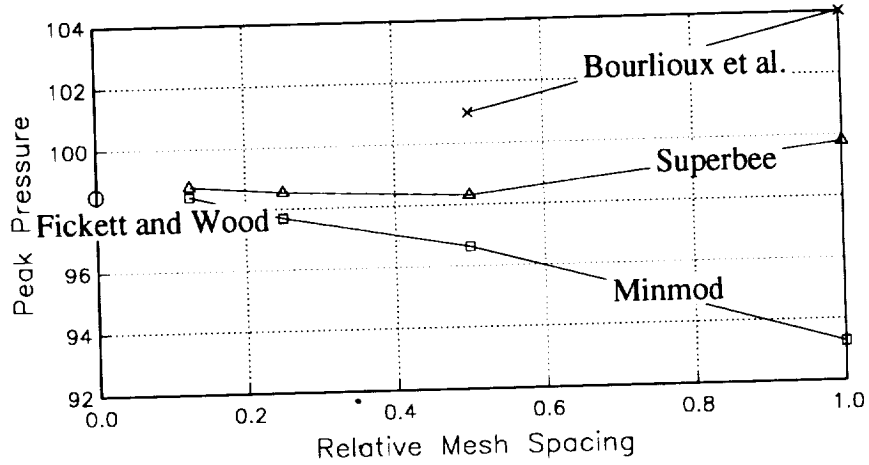

Figure 8: Variation of peak pressure with mesh spacing.

Even for this relatively simple problem, some numerical artifacts can occur if one is not careful. For example, at one stage in the cycle of the pulsating detonation, the profile for the reactant mass fraction is considerably steeper than the profile for the steady ZND detonation wave upon which the mesh spacing is based. Consequently, as shown by Figure 9, a grid which gives 10 mesh points for the half-reaction length of the ZND wave may at times give only half the expected number of cells for the pulsating front. For a compressive limiter function such as Superbee, if there are too few cells covering a steep but continuous profile, the profile will

appear as a smeared discontinuity that needs steepening. Hence an under-resolved profile is often artificially steepened by a compressive limiter. Here, such oversteepening causes anomalies to appear in the shock pressure history, see Figure 10. Note that such anomalies are not associated with the lead shock front, and so the question of whether the front is fitted or captured is immaterial.

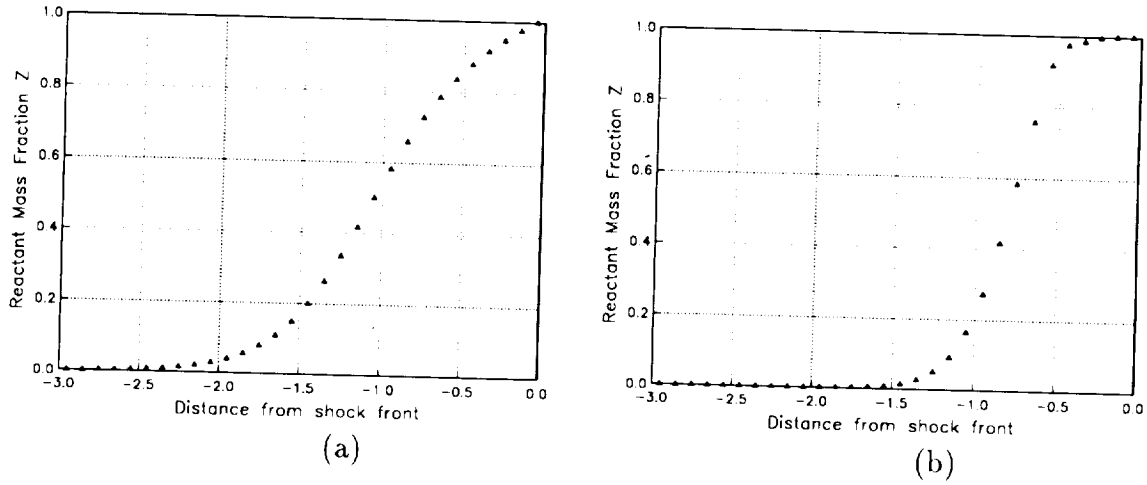

Figure 9: The reaction profile for a pulsating detonation wave may at times be considerably steeper than that for the initial steady ZND wave. (a) ZND wave. (b) Pulsating wave.

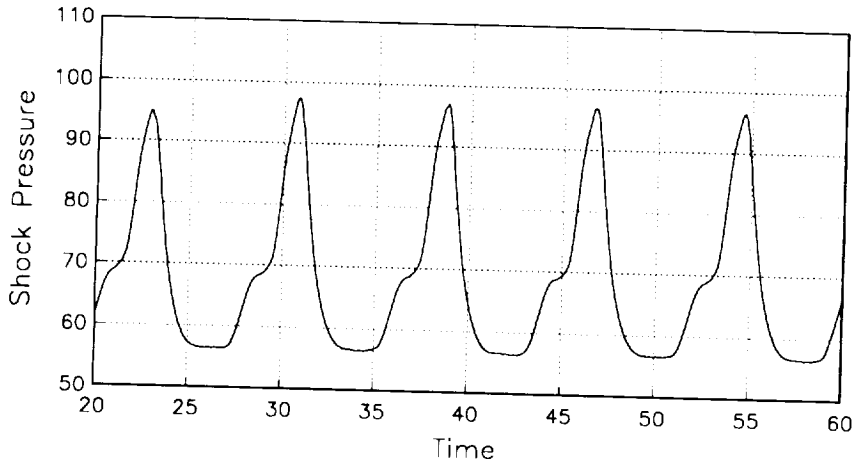

Figure 10: Anomalies often arise when an under-resolved calculation employs a compressive limiter function.

Following Bourlioux (1991) we have also conducted a two-dimen-sional test of our detonation code, namely, the simulation of the transverse waves, or so-called cellular structure, produced by a detonation wave travelling down a narrow channel. For this calculation the overdrive is 1.2, the channel width is 10 half-reaction lengths, and the dimensionless parameters are $\gamma = 1.2$, $q = 50$, $E^+ = 10$ and $K = 3.124$. The calculation was started with the solution for the ZND wave as initial data. This planar detonation front was perturbed by simply allowing it to ingest a small region of fluid where the rate constant K was artificially decreased by 20%. The calculation was then run until the ensuing transverse wave structure was fully developed, at which point a series of Schlieren-type images were taken so that we could compare our results with Bourlioux's. These Schlieren-type images are shown in Figure 11. Note that the calculation applied periodic boundary conditions along the top and the bottom of the channel and that here we have plotted four periods. Qualitatively, at least[3], these results compare well with Bourlioux's results, and all the salient features of the flow have been resolved (256 mesh cells covered the width of the channel). In particular, the regularity of the repeated vortex patterns are the same for both sets of calculations.

At this juncture, it is worth showing the results that were produced when we employed an exact Riemann solver rather than our adaptive Riemann solver, see Figure 12 (only one period is shown). As might be expected from having seen Figure 5 (d), spurious transverse waves are produced in the vicinity of the lead shock front. These spurious waves prevent the correct transverse wave structure from developing, thus ruining the simulation. It is our contention that most, if not all, of the Riemann solvers that are commonly employed would be similarly unable to *capture* the lead detonation front for this test problem. Whilst some may take this as reason enough why one should always fit the lead shock front, we have shown that if some care is taken, when it comes to detonation simulations, shock-capturing remains a viable alternative to shock-fitting.

In an attempt to unravel some of the dynamics of the detonation wave for this problem, we have rerun this test using a grid that was four times finer than before. In order to achieve such high grid resolutions we employ a relatively sophisticated mesh adaption scheme the details of which are too involved to give here (Quirk, 1991). Figure 13 presents a pair of Schlieren-type images for the temperature field which show the local flow structure just before, and just after, two triple points collide. It would appear that the collision gives rise to the familiar "explosion within an explosion", which in this case, because of the local shock structure, is highly anisotropic. This explosion causes slugs of hot fluid to be shot fore and aft giving rise to vortical structures which are similar to those associated with Rayleigh-Taylor instabilities. Note how the impact of the forward facing jet on the lead shock front causes the front to bulge.

Obviously, given the complexity of the flow field for this test problem there is little chance of validating every detail of the simulation. However, we feel that our computational method has matured to the point where it may be relied upon to provide simulations of sufficient fidelity for fathoming the details of complicated flow mechanisms as is done here.

[3]Owing to insufficient information, we are unable to perform a quantitative comparison.

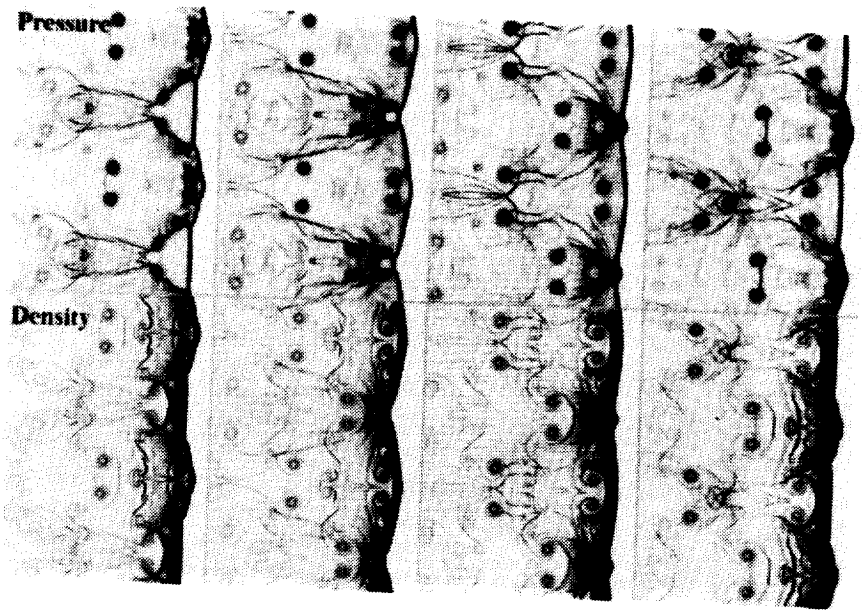

Figure 11: A sequence of four Schlieren-type snapshots which show the transverse wave structure of the detonation front.

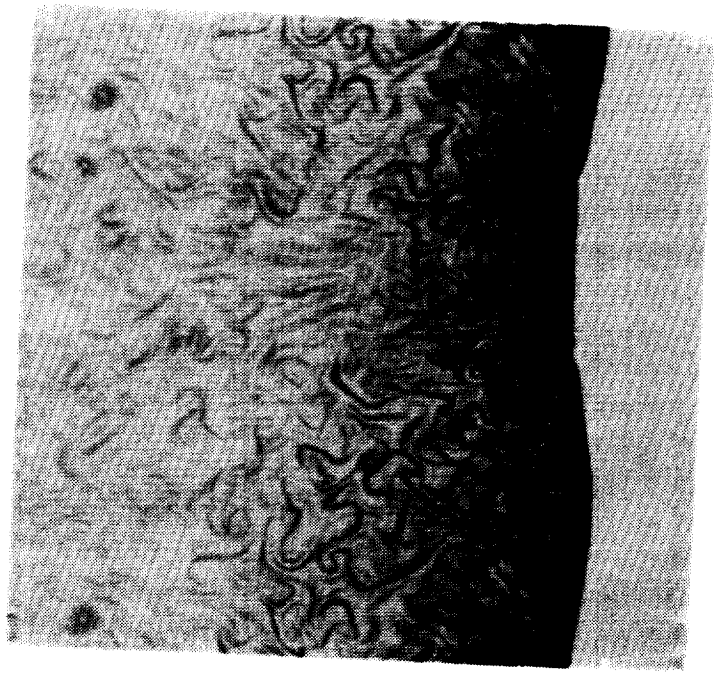

Figure 12: Spurious waves are produced, if the lead shock front is captured using an exact Riemann solver.

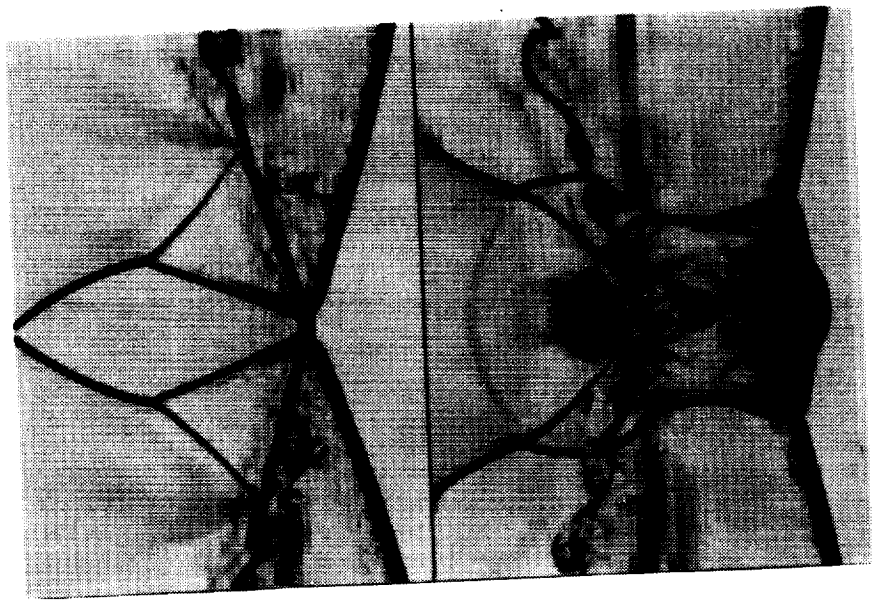

Figure 13: A pair of Schlieren-type images for the temperature field which show the sequence of events when two triple points collide.

6. Conclusions

In this paper, we have shown that Godunov-type schemes do not always live up to their reputation as being models of robustness. Specifically, the upwind dissipation provided by almost all Riemann solvers is inadequate for *capturing* detonation fronts in complex, multi-dimensional flows; a numerical instability can develop along the length of the detonation front which interferes with the genuine transverse waves associated with the propagation of the front. At the very least, we suggest that some artificial dissipation mechanism be used to augment the inherent upwind dissipation so as to suppress this type of numerical instability, albeit at a cost of some loss in resolution. In general, however, to improve the all-round robustness of a Godunov-type scheme without incurring any appreciable loss in resolution, we advocate the use of an adaptive Riemann solver. The shortcomings of any one preferred Riemann solver are circumvented by combining it with one or more complementary solvers, such that an individual Riemann solver is only used in the sorts of situations for which it is known to give reliable results. Admittedly this approach is not as straightforward to implement as would be the addition of an auxiliary dissipation mechanism to one's favourite Riemann solver, but it does prove to be an effective means for producing high fidelity simulations of detonation phenomena. As such, it provides an alternative means of simulating detonation phenomena for workers who might otherwise feel compelled to fit the detonation front solely in order to avoid the numerical difficulties associated with strong shocks.

References

Anderson, W.K., Thomas, J.L. and van Leer, B., 1985. "A comparison of finite-volume flux-vector splittings for the Euler equations,"AIAA paper 85-0122.

Bazhenova, T.V., Gvozdeva, L.G. and Nettleton, M.G., 1984. "Unsteady interactions of shock waves,"*Progress in Aerosp. Sci.* Vol. **21**, pp. 249-331.

Berger, M.J. and Colella, P., 1989. "Local adaptive mesh refinement for shock hydrodynamics,"*J. Comput. Phys.* **82**, pp. 64-84.

Bourlioux, A., 1991. "Numerical study of unstable detonations,"
Ph.D. Thesis, Princeton University, Princeton, NJ.

Bourlioux, A., Majda, A.J. and Roytburd V., 1991. "Theoretical and numerical structure for unstable one-dimensional detonations,"*SIAM J. Appl. Math.* **51**, No.2, pp. 303-342.

Colella, P. and Woodward, P.R., 1984. "The piecewise parabolic method (PPM) for gas-dynamical simulations,"*J. Comput. Phys.* **54**, pp. 174-201.

Einfeldt, B., 1988. "On Godunov-type methods for gas dynamics," *SIAM J. Numer. Anal.* **25**, No.2, pp. 294-318.

Fickett, W. and Wood, W.W., 1966. "Flow calculation for pulsating one-dimensional detonation,"*Phys. Fluids* **9**, pp. 903-916.

Harten, A., Enquist, B., Osher, S., and Chakravarthy, S.R., 1987. "Uniformly high order accurate essentially non-oscillatory schemes, III,"*J. Comput. Phys.* **71**, pp. 231-303.

Holt, M., 1984. "Numerical methods in fluid dynamics,"Springer, Berlin, 273 pp. 2nd ed.

Peery, K.M. and Imlay, S.T., 1988. "Blunt-body flow simulations,"
AIAA paper 88-2904.

Quirk, J.J., 1991. "An adaptive grid algorithm for computational shock hydrodynamics,"Ph.D. Thesis, College of Aeronautics, Cranfield Institute of Technology, U.K.

Quirk, J.J., 1992 *a*. "An alternative to unstructured grids for computing gas dynamic flows around arbitrarily complex two-dimensional bodies,"*ICASE Report No. 92-7*. In press, *Computers & Fluids*.

Quirk, J.J., 1992 *b*. "A contribution to the great Riemann solver debate,"*ICASE Report No. 92-64*. Submitted to *Int. J. Numer. Meth. Fluids*.

Roberts, T.W., 1990. "The behaviour of flux difference splitting schemes near slowly moving shock waves," *J. Comput. Phys.* **90**, pp. 141–160.

Roe, P.L., 1985. "Some contributions to the modelling of discontinuous flows," *Lecture Notes in Applied Mathematics.* **22**, Springer-Verlag, pp. 163–193.

Roe, P.L., 1986. "Characteristic-Based schemes for the Euler equations," *Ann. Rev. Fluid Mech.* **18**, pp. 337–365.

Toro, E.F., 1991. "A linearised Riemann solver for the time-depend-ent Euler equations of gas dynamics," *Proc. Roy. Soc. London* A **434**, pp. 683–693.

*U.S. GOVERNMENT PRINTING OFFICE: 1993-728-150/60035

REPORT DOCUMENTATION PAGE

Form Approved
OMB No 0704-0188

1. AGENCY USE ONLY (Leave blank)	2. REPORT DATE	3. REPORT TYPE AND DATES COVERED
	April 1993	Contractor Report

4. TITLE AND SUBTITLE
GODUNOV-TYPE SCHEMES APPLIED TO DETONATION FLOWS

5. FUNDING NUMBERS
C NAS1-19480

WU 505-90-52-01

6. AUTHOR(S)
James J. Quirk

7. PERFORMING ORGANIZATION NAME(S) AND ADDRESS(ES)
Institute for Computer Applications in Science and Engineering
Mail Stop 132C, NASA Langley Research Center
Hampton, VA 23681-0001

8. PERFORMING ORGANIZATION REPORT NUMBER
ICASE Report No. 93-15

9. SPONSORING / MONITORING AGENCY NAME(S) AND ADDRESS(ES)
National Aeronautics and Space Administration
Langley Research Center
Hampton, VA 23681-0001

10. SPONSORING / MONITORING AGENCY REPORT NUMBER
NASA CR-191447
ICASE Report No. 93-15

11. SUPPLEMENTARY NOTES
Langley Technical Monitor: Michael F. Card
Final Report

To appear in the Proceedings of the 2nd ICASE/NASA LaRC Combustion Workshop, October 12-14, 1992

12a. DISTRIBUTION / AVAILABILITY STATEMENT
Unclassified - Unlimited

Subject Category 02,64

12b. DISTRIBUTION CODE

13. ABSTRACT *(Maximum 200 words)*

Over recent years, a variety of shock-capturing schemes have been developed for the Euler equations of gas dynamics. During this period, it has emerged that one of the more successful strategies is to follow Godunov's lead and utilize a nonlinear building block known as a Riemann problem. Now, although Riemann solver technology is often thought of as being mature, there are in fact several circumstances for which Godunov-type schemes are found wanting. Indeed, one inherent deficiency is so severe that if left unaddressed, it could preclude such schemes from being used to capture detonation fronts in simulations of complex flow phenomena. In this paper, we highlight this particular deficiency along with some other little known weaknesses of Godunov-type schemes, and we outline one strategy that we have used to good effect in order to produce reliable high resolution simulations of both reactive and nonreactive shock wave phenomena. In particular, we present results for simulations of so-called galloping instabilities and detonation cell phenomena.

14. SUBJECT TERMS	15. NUMBER OF PAGES
Godunov schemes, detonation flows	20
	16. PRICE CODE A03

17. SECURITY CLASSIFICATION OF REPORT	18. SECURITY CLASSIFICATION OF THIS PAGE	19. SECURITY CLASSIFICATION OF ABSTRACT	20. LIMITATION OF ABSTRACT
Unclassified	Unclassified		